

Quantifying variance due to temporal and spatial difference between ship and satellite winds

Jackie C. May^{1,2,3} and Mark A. Bourassa^{1,2}

Received 3 January 2011; revised 3 May 2011; accepted 17 May 2011; published 19 August 2011.

[1] Ocean vector winds measured by SeaWinds can be validated with comparison in situ data that are within a certain time and space range to the satellite overpass. The total amount of random observational error is composed of two primary components, which are quantified in this study: the uncertainty associated with the data sets and the uncertainty associated with the temporal and/or spatial difference between two observations. The variance associated with a temporal difference, which can be translated into a spatial difference using Taylor's hypothesis, between two observations is initially examined in an idealized case that includes only Shipboard Automated Meteorological and Oceanographic System (SAMOS) 1 min data. The results show that the amount of variance in wind speed and direction increases as the time difference increases, while the amount of variance in wind speed increases and direction decreases with larger wind speeds. Collocated SeaWinds and SAMOS observations are used to determine the total amount of variance associated with a temporal (equivalent) difference from 0 to 60 min. For combined differences less than 25 min (equivalent) and the selected wind speed bins, the variance associated with the temporal and spatial difference is dominated by small changes in the wind speed distribution, and the sum of the observational errors is approximately $1.0 \text{ m}^2 \text{ s}^{-2}$ (12 deg^2) and $1.5 \text{ m}^2 \text{ s}^{-2}$ (10 deg^2) for wind speeds between 4 and 7 m s^{-1} and $7\text{--}12 \text{ m s}^{-1}$. For larger combined differences, the observational error variance is no longer the dominant term; therefore, the total variance is seen to gradually increase with increasing time differences.

Citation: May, J. C., and M. A. Bourassa (2011), Quantifying variance due to temporal and spatial difference between ship and satellite winds, *J. Geophys. Res.*, 116, C08013, doi:10.1029/2010JC006931.

1. Introduction

[2] Ocean surface wind vectors are important in many applications, including weather prediction, understanding dynamical forcing of the ocean, and studying air-sea interactions and climate [Huddleston and Spencer, 2001; Liu, 2002; Bourassa et al., 2010b]. Scatterometers, radar altimeters, synthetic aperture radars (SAR), microwave radiometers, and in situ observations provide different methods of obtaining wind speeds, and in some cases directions, globally over the ocean; however, scatterometers have proven to be the most effective instrument for retrieving ocean surface vector winds [Liu and Xie, 2006]. The primary purpose of spaceborne microwave scatterometers, such as the SeaWinds scatterometer onboard the QuikSCAT satellite, is to provide frequent global wind measurements over the ocean.

[3] Several studies [Stoffelen, 1998; Freilich and Dunbar, 1999; Ebuchi et al., 2002; Bourassa et al., 2003] have shown that collocated in situ observations can be used to calibrate and validate scatterometer wind vectors. Ideally, the in situ observations used for comparisons would be collocated in both time and space with the satellite overpass. In reality, however, these ideal collocations are rare. Two reasons for nonideal collocations are that in situ data are sparse and the in situ sampling interval is large compared to the high along-track temporal sampling frequency of SeaWinds. To partially compensate for the lack of ideally collocated comparison observations, observations used for comparison are limited to those that are within a certain time and space range of the satellite overpass. In a comparison of these two data sets, additional uncertainty due to the temporal and/or spatial difference between the two observations should be considered along with the uncertainty associated with the data sets. The data set uncertainty includes instrument noise from both the scatterometer and the in situ measurements, incorrect ambiguity selection by the scatterometer, motion from the in situ measurement platform, time averaging, and human error from manual in situ observations [Pierson, 1990; Chen, 2000]. In this study, the amount of error associated with the temporal and spatial difference

¹Center for Ocean-Atmospheric Prediction Studies, Florida State University, Tallahassee, Florida, USA.

²Department of Earth, Ocean and Atmospheric Science, Florida State University, Tallahassee, Florida, USA.

³Now at QinetiQ North America, Stennis Space Center, Mississippi, USA.

between SeaWinds and in situ-measured winds will be quantified, as well as the amount of error associated with the data sets.

[4] Previous studies have had many limitations when examining the error difference for comparing in situ buoy observations with either altimeter or scatterometer data. *Dobson et al.* [1987] used hourly buoy observations and altimeter data that were assessed along the satellite surface track every 7 km to determine the overall wind speed root mean square (rms) error difference to be 1.7 m s^{-1} for all collocations within a 30 min and 50 km range. *Monaldo* [1988] used hourly buoy observations and altimeter data to examine the error dependency for temporal differences in 1 h increments and spatial differences in 5 km increments. The total expected RMS error difference for all wind speed comparisons with an average difference of 15 min and within a 50 km range was found to be 1.8 m s^{-1} . *Kent et al.* [1999] used pairs of voluntary observing ship (VOS) observations with the same reporting hour and within 300 km to determine the random observational error variance for the 10 m corrected wind speed to range from 1.3 to 2.8 m s^{-1} . The study by *Chen* [2000] included only numerical simulations to find the optimal temporal and spatial windows of 6–12 min and 10–20 km, respectfully; however, no real world validation was performed. Different sources of uncertainty, including spatial difference, between SeaWinds and research vessel observations were identified and examined by *Bourassa et al.* [2003]. The wind vector uncertainty was examined as a function of the spatial difference between the research vessel and SeaWinds observations; however, the variance associated with the temporal difference was not considered.

[5] The spatial and temporal resolutions used to examine the variance in this study are much finer than those used by other studies. This study will focus on temporal differences between observations of less than 30 min and spatial differences between observations of less than 30 km. Selecting smaller ranges of acceptable temporal and spatial differences allows the total amount of variance associated with comparing two data sets to be examined as a function of the combined temporal and spatial difference. Another limitation of the previous studies is that only a few months of data were used for analysis; the more extensive data set used herein, including data from all months of the year for 5 years, provides more robust results. Many of the previous studies also ignored the additional error caused by a changing sea state, which could contribute a significant amount to the total error. Last, the in situ data set used in this study consists of quality controlled observations from research vessels. These observations are usually more accurate than buoy or VOS observations [*Smith et al.*, 1999], which have been used in many of the previous studies.

[6] The amount of uncertainty that can be attributed to a temporal and spatial difference between two wind observations is determined in this study by using an idealized case in which only in situ data are considered. In situ data are obtained from the Shipboard Automated Meteorological and Oceanographic System (SAMOS) initiative and consist of measurements collected at 1 min intervals over the period 2005–2009. For this idealized scenario, the satellite is assumed to pass directly over the ship every hour on the hour. Shifts of time from the assumed satellite overpass are

used to examine the error associated with a mismatch in time. Taylor's hypothesis (frozen turbulence) [*Taylor*, 1938] can then be used to translate a temporal shift to a spatial shift. This uncertainty is also examined as a function of wind speed.

[7] The second part of this study verifies the results from the first part using collocated SAMOS and SeaWinds observations. The total amount of random observational variance between the two observations is examined as a function of the spatial/temporal difference as well as a function of wind speed. The total variance can be separated into two components: the variance associated with a temporal and spatial difference between two observations and the variance associated with the data sets. This separation allows for each of these variance components to be examined and quantified individually.

[8] Knowing the variance associated with the temporal and spatial difference between two observations and the variance associated with the two data sets is useful in the calibration of other instruments, data assimilation, operational numerical weather prediction, development of geophysical model functions, and creation of gridded products [*Liu*, 2002; *Bourassa et al.*, 2003]. The method presented in this analysis uses SeaWinds and SAMOS wind observations. Although SeaWinds recently ceased to function, it provided an extensive data set to work with and the results will be useful in reanalysis efforts. Also, the method presented in this analysis can be applied to any data set; it is not limited to only SeaWinds and SAMOS observations.

[9] The conversion of in situ winds to equivalent neutral winds (the "winds" observed by satellite) is explained in section 2. The data used in this conversion and for the comparison (SeaWinds, SAMOS, wave, and current data) are also described. The method used to determine the amount of variance as a function of space or time and wind speed in an idealized scenario is discussed in section 3. In section 4, the procedure for collocating the SeaWinds measurements, SAMOS observations, wave, and current data is described. Finally, the amount of uncertainty due to the temporal and spatial difference between the SeaWinds and SAMOS observations, as well as the amount of uncertainty associated with the data sets, is determined as a function of time and wind speed. These results are presented in section 5.

2. Data

2.1. Equivalent Neutral Winds

[10] Scatterometers operate by sending microwave pulses to the ocean surface and measuring the backscatter cross section from the surface roughness. The ocean surface is modified by surface capillary waves caused by wind stress [*Weissman et al.*, 1994; *Bourassa et al.*, 1999; *Liu and Xie*, 2006]. The wind stress is then calibrated into an "equivalent neutral" (EN) wind speed at a reference height of 10 m [*Ross et al.*, 1985; *Weissman et al.*, 1994; *Portabella and Stoffelen*, 2009; *Bourassa et al.*, 2010a].

[11] The in situ comparison observations from SAMOS, used to validate the scatterometer measurements, must also be height adjusted to 10 m and then converted from actual winds into EN winds. First, the SAMOS measured wind speeds are translated into true winds using the method

described by *Smith et al.* [1999]. This alteration removes the ship motion from the recorded wind speed. If the ship motion is not removed, additional errors in wind comparisons arise, especially when averaging the SAMOS data over any amount of time. Next, to adjust the actual wind speed measured at a given anemometer height to a reference height (z) of 10 m, the following equation for the modified log wind profile (equation (1)) is used

$$U(z) - U_{sfc} = \frac{u_*}{\kappa} \left[\ln \left(\frac{z}{z_0} + 1 \right) - \varphi(z, z_0, L) \right], \quad (1)$$

where the surface friction velocity (u_*) is the square root of the kinematic stress (τ/ρ), τ is the surface wind stress, ρ is the density of the air, z_0 is the momentum roughness length, U is the wind speed at height z , U_{sfc} is the wind speed at the ocean surface, κ is the von Kármán's constant ($\kappa = 0.4$), φ is an atmospheric stability term, and L is the Monin-Obukhov scale length. Traditionally, EN winds differ from actual winds in that they assume neutral stratification in the atmosphere ($\varphi = 0$), but use the nonneutral values of u_* and z_0 determined from equation (1) and a reference height of 10 m. This approach was designed to allow the correct stress to be calculated from the equivalent neutral wind and a neutral drag coefficient.

[12] *Bourassa et al.* [2010a] presented a revised definition for 10 m EN wind (U_{10EN}) that includes a density adjustment term, equation (2)

$$U_{10EN} - U_{sfc} = \frac{u_*}{\kappa} \left[\ln \left(\frac{z}{z_0} + 1 \right) \right] \sqrt{\frac{\rho}{\rho_0}}, \quad (2)$$

where ρ_0 is standard reference density of air set at 1.0 kg m^{-3} . This adjustment is typically less than 5% of the wind speed and is necessary because an air density dependent error was found in the comparison of satellite and in situ equivalent neutral winds. This modification is also consistent with the concept of a scatterometer responding (indirectly) to surface stress as opposed to the friction velocity. A boundary layer model [*Bourassa, 2006*] based on the *Bourassa, Vincent, and Wood (BVW)* model [*Bourassa et al., 1999*] is used to adjust the in situ measured winds to U_{10EN} winds.

2.2. SeaWinds Scatterometer

[13] The SeaWinds microwave scatterometer onboard the polar-orbiting QuikSCAT satellite was launched into space on 19 June 1999. Initially, its mission was to continue scatterometer coverage after the payload malfunction of the Advanced Earth Observing Satellite (ADEOS-I), until ADEOS-II could be launched. Unfortunately, ADEOS-II was operational for only 6 months. QuikSCAT, on the other hand, remained operational until late 2009. It provided over 10 years of continuous global coverage and has proven to be beneficial to both operational and research efforts.

[14] SeaWinds operated in the microwave band at 13.4 GHz using two rotating pencil beam antennas. The inner beam was horizontally polarized with an incidence angle of 46.25° and a radius of 707 km, whereas the outer beam was vertically polarized with an incidence angle of 54° and a radius of 900 km. By operating in the microwave band, SeaWinds was able to sample the Earth's surface in both clear and cloudy conditions throughout the day and night. There were between

8 and 20 radar cross sections (footprints) that were combined into $25 \times 25 \text{ km}$ wind cells. The center of each wind cell was the center of mass of all of the footprints within that cell. Up to 76 wind cells composed the 1800 km wide observation swath, with the most accurate observations found between 200 and 700 km from nadir [*Bourassa et al., 2003*]. Subsequent reprocessing resulted in the regions of higher quality data being extended much closer to nadir.

[15] The SeaWinds version 3 swath data produced by the Remote Sensing Systems, reprocessed to add updated radiometer data to the files, are used in this study. The Ku-2001 geophysical model function was used to retrieve the wind data. The SeaWinds wind data and additional details are available online from the Remote Sensing Systems (<http://www.remss.com>).

[16] One of the limitations of scatterometers, is that rain can have adverse effects on the scatterometer wind retrieval process. Rain can alter the radar signal through scattering and two-way attenuation. Also, sea surface roughness is changed by the impact of the raindrops [*Weissman et al., 2002; Bourassa et al., 2003; Draper and Long, 2004*]. The SeaWinds data set obtained from the Remote Sensing Systems contains several rain flags that are used to identify seriously rain contaminated scatterometer data, and data for which there are insufficient radiometer observations to provide a radiometer-based flag. As suggested by Remote Sensing Systems, data identified with the following flags have been omitted from this study: expected quality of the vector retrieval (`iclass`) = 0 (no retrieval), scatterometer rain flag (`irain_scat`) = 1 (indicates rain), radiometer rain rate (`rad_rain`) > 0.15, and time difference between scatterometer and collocated radiometer (`min_diff`) > 30.

[17] Another limitation of scatterometers is ambiguity selection. Because of the design and wind retrieval process of scatterometers, a unique wind direction must be selected from one or more likely solutions. This process is called ambiguity selection. For wind speeds less than 3 m s^{-1} , SeaWinds is known to have some ambiguity selection error [*Bourassa et al., 2003*]. Incorrectly chosen ambiguities are eliminated from the real world comparisons in sections 4 and 5.

2.3. SAMOS Data

[18] One of the most commonly used type of in situ data for scatterometer comparisons are research vessel data. *Pierson* [1990] concluded that ship reported wind data are of poor quality for several reasons, including: human estimated winds were often estimated to the nearest 5 knots and to eight points of the compass, ships could report wind speed only in integers, typographical errors in ship reports, not accounting for ship motion, and poorly educated observers. Ships that are part of the Voluntary Observing Ship (VOS) project may still have some of the above mentioned errors associated with the data; however, data collected through the SAMOS initiative eliminate these errors. The SAMOS initiative is complementary to the VOS project, with a few key differences. A SAMOS automatically records navigational, meteorological, and oceanographic parameters with a computerized data logging system at 1 min intervals [*Smith et al., 2010*]. VOS observations are reported every 1–6 h and could be either manual or automated measurements. The instruments on SAMOS equipped research vessels tend to be better

Table 1. Recorded Parameters by SAMOS With Their Respective Units and Accuracy^a

Variable	Units	Accuracy of Mean
Ship position	latitude, longitude (deg)	0.001°
Ship course over ground	deg (clockwise from true north)	2°
Ship speed over ground	knots	larger of 2% or 0.2 m s ⁻¹ (0.4 knots)
Ship heading	deg (clockwise from true north)	2°
Ship-relative wind speed	m s ⁻¹	larger of 2% or 0.2 m s ⁻¹ (0.4 knots)
Ship-relative wind direction	deg (clockwise from bow)	3°
Earth-relative (true) wind speed	m s ⁻¹	larger of 2% or 0.2 m s ⁻¹ (0.4 knots)
Earth-relative (true) wind direction	deg (clockwise from true north)	3°
Air temperature	°C	0.2°C
Atmospheric pressure	mb	0.1 mb
Relative humidity	%	2%
Precipitation	mm d ⁻¹	~0.4 mm d ⁻¹
Radiation	W m ⁻²	5 W m ⁻²
Sea temperature	°C	0.1°C

^aMetadata on the location and type of instrument are also available.

sited and maintained than instruments on typical VOS platforms. Although the VOS project has much denser spatial coverage because it includes more vessels, SAMOS has a much higher temporal sampling, which is more advantageous to some research topics.

[19] The other most commonly used comparison in situ data type are buoy data. Buoy winds are typically reported every 10 or 60 min. Compared to winds measured by SAMOS, buoy winds are more intermittent (albeit more plentiful in space), modifications caused by the sea state are more problematic [Bourassa *et al.*, 2003], and the operational buoys are less well calibrated. Therefore, in situ data used in this study are composed of the data collected through the SAMOS initiative. The SAMOS initiative became operational as of 2005, and the data are available online from the Research Vessel Surface Meteorology Data Center (http://samos.coaps.fsu.edu/html/data_availability.php). The recorded parameters are given in Table 1, along with their respective units and accuracy [Bradley and Fairall, 2006].

[20] Eight SAMOS-equipped research vessels are used in this study. The research vessel name, anemometer height, location of cruise track, dates of available data, and total number of acceptable observations are given in Table 2. The spatial range of these ships includes the Atlantic, Pacific, Gulf of Alaska, Southern Ocean, and Arctic Ocean. All

seasons of the year in both hemispheres are represented. Since many different geophysical conditions are sampled in this study, there is unlikely to be a bias due to a particular location or time of year.

[21] The version 200 SAMOS data, which have undergone common formatting, metadata enhancement, and automated quality control [Smith *et al.*, 2010], are used in this study. Version 200 data have been compacted into daily files and are available from 2005 onward. Although this data set has not undergone visual inspection or further quality control it is the most complete SAMOS data set currently available. To make the SAMOS-recorded winds comparable to SeaWinds observations, the winds are adjusted to U_{10EN} using the method discussed in section 2.1.

2.4. Ocean and Current Data

[22] Scatterometers respond to the ocean surface roughness, which is modified by the wind stress. Surface stress is primarily dependent on the wind shear [Bourassa, 2004]. Therefore, scatterometer-measured wind speeds are more closely related to the wind shear than they are to the equivalent neutral wind speed at 10 m. By including the horizontal motion of the ocean surface due to ocean waves and currents with the SAMOS-determined 10 m EN wind speeds, more accurate surface-relative in situ comparison data can be obtained. Model wave and current data are used in this study to represent the ocean surface. The model outputs are bilinearly interpolated to the location of the research vessel winds.

[23] The ocean wave data used in this study were obtained from the global National Oceanic and Atmospheric Administration (NOAA) WAVEWATCH III (NWW3) ocean wave model. The spatial coverage of this model is from 77°S to 77°N, with a 1.25° longitudinal and 1.0° latitudinal grid spacing. The temporal resolution is every 3 h. Output from this model includes zonal and meridional wind speed, significant wave height, peak wave period, and peak wave direction. Additional details about the model are available online from NOAA (<http://polar.ncep.noaa.gov/waves/implementations.shtml>).

[24] The ocean current data used in this study were obtained from the Ocean Surface Current Analyses - Real Time (OSCAR) global data set from NOAA. OSCAR data provide operational ocean surface velocity, or currents, from satellite fields [Bonjean and Lagerloef, 2002]. Both the zonal and meridional ocean surface currents are given from 69.5°S to 69.5°N on a global 1.0° by 1.0° grid spacing at approximately 5 day intervals. Further details of this project

Table 2. Vessels Used in Idealized Case and Comparison Observations With SeaWinds

Research Vessel	Anemometer Height (m)	Location	Available Data	Total Number of Observations
<i>Atlantis</i>	19.8	North Atlantic and North Pacific	June 2005 to November 2009	1,636,996
<i>David Star Jordan</i>	19.8	North Pacific	March 2008 to April 2009	197,693
<i>Healy</i>	30.9	Gulf of Alaska and Arctic Ocean	June 2007 to October 2009	502,268
<i>Henry B. Bigelow</i>	15.0	North Atlantic	April 2007 to November 2009	415,643
<i>Knorr</i>	15.5	Atlantic and Pacific	May 2005 to November 2009	1,808,340
<i>Laurence M. Gould</i>	30.5	Southern Ocean	April 2007 to November 2009	970,432
<i>Miller Freeman</i>	22.8	Gulf of Alaska	January 2007 to October 2009	637,122
<i>Southern Surveyor</i>	24.0	South Pacific	April 2008 to November 2009	302,224

can be found online at the NOAA Web site (<http://www.oscar.noaa.gov>).

3. Idealized Scenario

3.1. Method

[25] This idealized study is designed to examine the natural variability associated with a temporal difference between two observations. Only the temporal difference will be considered here; there is assumed to be no spatial difference. Four parameters will be examined in this idealized scenario: actual wind speed (U_{10}), 10 m EN wind speed (U_{10EN}), wind direction, and wind stress. The variance of these parameters will be determined as both a function of the temporal difference as well as a function of wind speed.

[26] In this idealized case only in situ data are considered: the 1 min observations collected through the SAMOS initiative from 2005 to 2009. A pseudosatellite is assumed to pass directly over the ship every hour on the hour; therefore, every hourly SAMOS observation is considered an ideal collocation in both time and space to the pseudosatellite overpass. To match the sampling of SAMOS to a satellite, a time-averaging window is defined using Taylor's hypothesis [Taylor, 1938], or frozen turbulence. Frozen turbulence means that characteristics of the turbulence are "frozen" in time. Taylor's hypothesis allows for a spatial dimension to be converted to a temporal dimension, and vice versa. To easily understand this concept, one can apply it to the driving difference between two cities. For example, the interstate driving distance between Tallahassee, Florida, and Mobile, Alabama, is approximately 250 miles. If someone drives 70 miles h^{-1} on the interstate, then it would take that person roughly 3.5 h (distance/speed) to drive that distance. Therefore, the driving difference between the two cities can be expressed as either a spatial difference or temporal difference.

[27] Taylor's hypothesis is used to define a time-averaging window (t_{win}) centered on the hourly observation, equation (3). For a given volume of air (*footprint*) and speed at which it is traveling (\bar{U}), it is possible to determine how long (t_{win}) it would take to sample the total given volume

$$t_{win} = \frac{\text{footprint}}{|\bar{U}|}, \quad (3)$$

where *footprint* is the SeaWinds footprint size ($\text{footprint} = 7$ km) and \bar{U} is the average wind speed within the time-averaging window. As discussed in section 2.2, SeaWinds footprints were binned into 25×25 km cells; however, it has been shown that scatterometer sampling characteristics are better matched to winds on much smaller spatial scales [Long, 2002; Bourassa et al., 2003]. Bourassa et al. [2003] determined the balance between signal and noise in the research vessel observations best matches the scatterometer winds at a spatial-temporal scale of approximately 5 km. A spatial scale of 7 km was determined as the best match by D. Long (personal communication, 2003). The study presented here, like the study by Bourassa et al. [2003], contains research vessel and scatterometer observations; therefore, a footprint size of 7 km, instead of 25 km, is used for the remainder of the study.

[28] The size of the time-averaging window varies based on the average wind speed within that time-averaging

window. Low wind speeds correspond with large time-averaging windows, and high wind speeds correspond with small time-averaging windows. The average wind speed within each window, however, cannot be determined unless the size of the time-averaging window is known. Therefore, an iterative process is used starting with a first guess of 5 min for the time-averaging window. The average wind speed within this 5 min time-averaging window is then calculated to obtain a new time-averaging window, using equation (3). This process is repeated until a steady solution, when two consecutive time-averaging windows are within 1.5 min of each other, is obtained. If a stable solution is not found, that hourly observation is omitted from the idealized case data set. The new time-averaging window is assumed to be the time-averaging window centered on the hourly observation, thus representing an ideal collocation. Because wind speed varies with time, a fixed time-averaging window cannot be used for every hour. Therefore, this iterative process is replicated for each hour in the SAMOS data set.

[29] For each hour, the average U_{10} , U_{10EN} , wind direction, and wind stress are calculated within the corresponding time-averaging window. Since SAMOS records actual wind speed and direction, the average wind speed and average wind vector can be calculated easily. The average wind direction uses the direction associated with the vector averaged SAMOS winds. As discussed in section 2, all of the 1 min SAMOS wind speed observations are translated into EN wind speeds at 10 m using the BVW model; therefore, the average EN wind speed within each time-averaging window also can be obtained easily. Part of the translation from the anemometer recorded wind speed to EN wind speed includes calculating the surface wind stress using the observed atmospheric stability. As a result, the wind stress for each 1 min observation is known, which allows for the average wind stress within each time-averaging window to be calculated also.

[30] To represent comparison data that are not ideally collocated in time to the pseudosatellite, the center of the hourly time-averaging window is shifted away from the hourly observation in 1 min increments. The size of the time-averaging window remains the same as it is shifted. For each 1 min shift, new average values are determined within the shifted time-averaging window.

[31] The variance (σ_j^2) of all of the observations with a j min time shift is calculated from the difference between the hourly averages ($\bar{U}_{i,j=0}$) and the time-shifted averages ($\bar{U}_{i,j}$) for each 1 min shift using equation (4)

$$\sigma_j^2 = \frac{1}{N_j - 1} \sum_{i=1}^{N_j} (|\bar{U}_{i,j} - \bar{U}_{i,j=0}|)^2, \quad (4)$$

where N is the number of observations with a j min time shift. Equation (4) shows the calculation for the variance of the difference in earth-relative wind speed; however, the same method is used for all of the parameters discussed here. In addition to determining the variance of the differences as a function of the time difference from 0 to 60 min, it is also possible to examine the variance of the differences as a function of wind speed. The wind speed is grouped into intervals of 4 $m s^{-1}$. For example, in the first group, the wind speed ranges from 0 to 4 $m s^{-1}$, in the second group, the wind

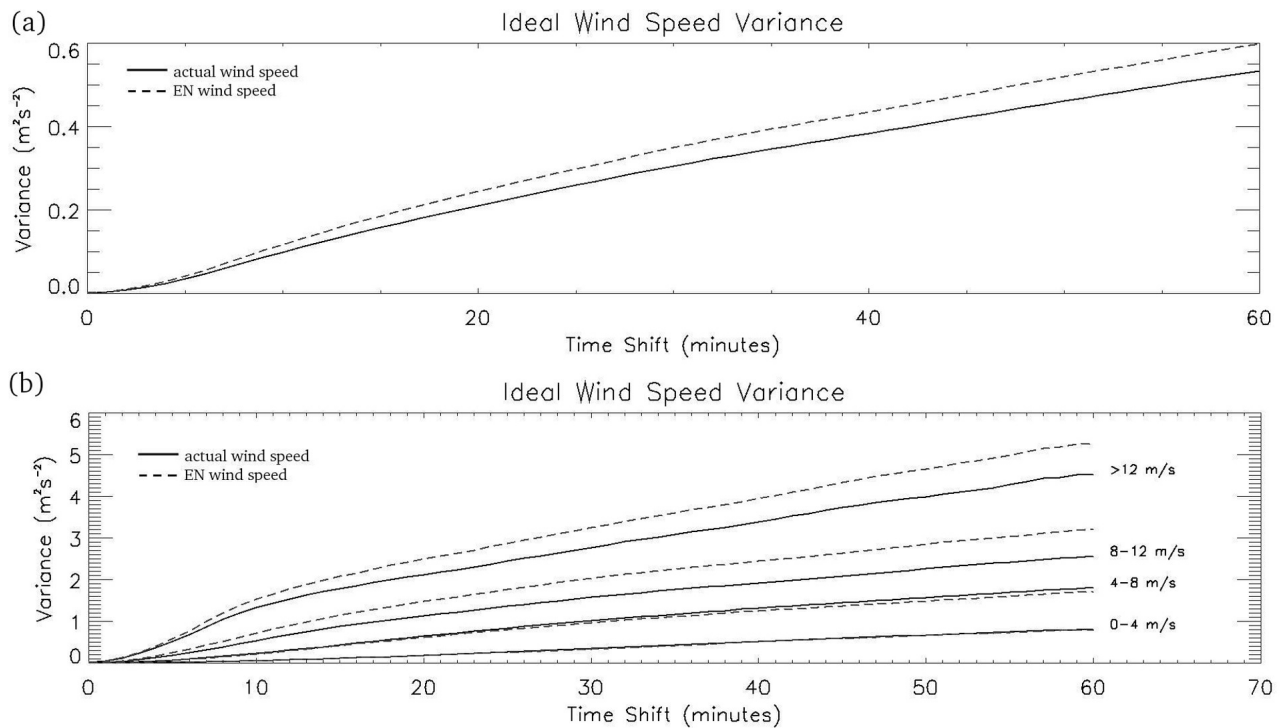


Figure 1. Variance of the differences in actual wind speed (solid lines) and 10 m EN wind speed (dashed lines) as a function of (a) miscollocation in time and (b) miscollocation in time and wind speed.

speed would range from 4 to 8 m s^{-1} , and so on. This method allows for examination of wind speed dependence of the variance.

3.2. Results

[32] The variance of the differences of U_{10} and of $U_{10\text{EN}}$ is examined as a function of the time difference from 0 to 60 min (Figure 1a) as well as a function of wind speed (Figure 1b). Figure 1a shows that the variance of the differences of each of these parameters begins at zero with a 0 min time difference, which would represent a perfect collocation and would therefore not have any miscollocation variance associated with it. Then the variance of the differences gradually increases as the time difference between two observations increases. The increasing trend is due to the fact that wind speed changes rapidly with time. The larger the time difference is between two observations, the greater the RMS difference in wind speed would be. The larger the wind speed difference is, the larger the variance of the difference in wind speed would be. It should also be noted in Figure 1a that the total variance of the differences of $U_{10\text{EN}}$ is slightly greater than the total variance of the differences of U_{10} . This characteristic can be explained by the typically unstable atmosphere found over the ocean: the ocean surface temperature is commonly warmer than the air temperature above. For unstable atmospheric conditions, EN winds, which are a better comparison to wind stress than actual winds, are stronger than actual winds [Kara *et al.*, 2008], and the variability in wind increases as the wind speed increases, as can be seen in Figure 1b. The U_{10} results shown in Figure 1a agree well with the results found by *Monaldo* [1988], who used wind

speed data from two buoys separated by time to find the associated variance.

[33] The same general trends seen in Figure 1a are seen for each wind speed group in Figure 1b. Also seen in Figure 1b is that the larger the wind speed, the greater the associated variance of the differences. The highest wind speed group (>12 m s^{-1}) is seen to have a more significant increase in the variance of the differences than the other three wind speed groups have. This increase is a result of the wind speed distribution within this wind speed group; there is a much broader range of wind speeds sampled in this group compared to the other 4 m s^{-1} groups. When the variance of the differences is split into wind speed groups, not every group shows the variance of the differences of $U_{10\text{EN}}$ being greater than the variance of the differences of U_{10} . As discussed before, the atmosphere is typically unstable over the ocean. Changes in wind speed in unstable conditions are associated with two resulting processes that partially compensate for each other. An increased wind speed results in more wind shear and hence more stress. However, the increased wind speed also causes more mechanical mixing, which leads to a more stable atmosphere; a more stable atmosphere is associated with less wind stress [Kara *et al.*, 2008]. These effects can be seen in Figure 1b with the different wind speed groups. For low to moderate wind speeds, changes in $U_{10\text{EN}}$ are compensated for by the associated changes in atmospheric stability; therefore, the variability associated with $U_{10\text{EN}}$ is approximately equal to that of U_{10} in the two lowest wind speed groups. For larger wind speeds, the atmospheric stability has less influence and cannot compensate for the greater variability associated with the larger wind speeds. Therefore, the variability associated with

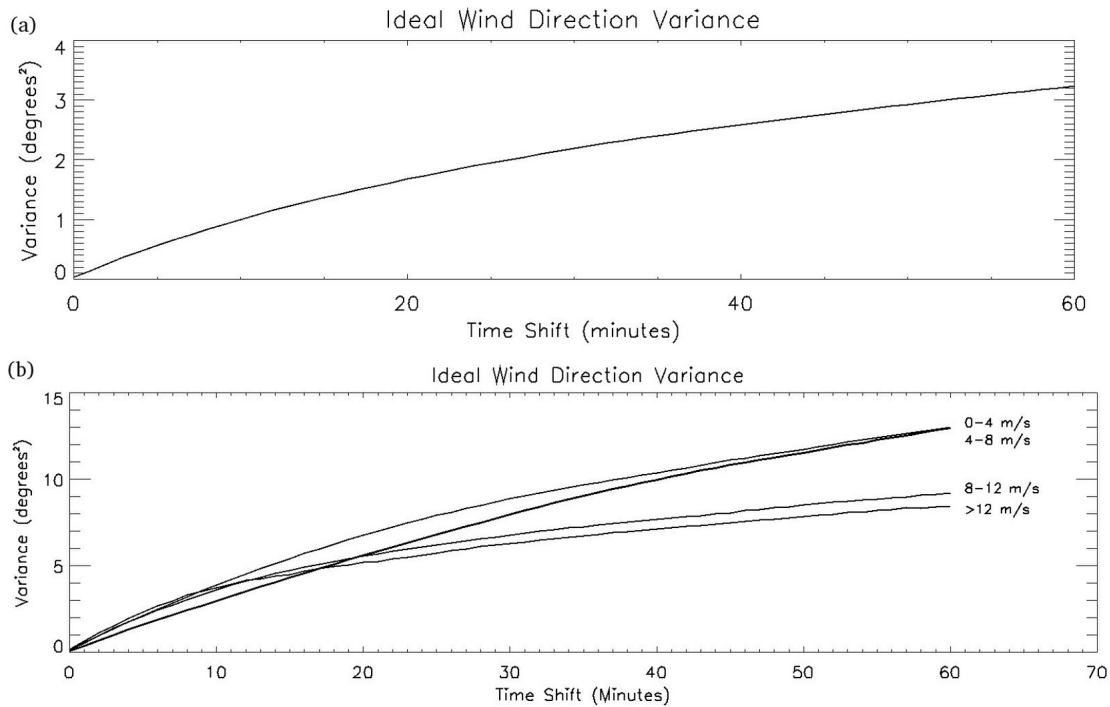


Figure 2. Variance of the differences in wind direction as a function of (a) miscollocation in time and (b) miscollocation in time and wind speed.

U_{10EN} is greater than that of U_{10} in the higher wind speed groups.

[34] Figure 2 shows the variance of the differences of wind direction. Similar to the variance of the differences of wind speed, the variance of the differences of wind direction begins at zero with a 0 min time difference and then increases as the time difference increases (Figure 2a). As discussed previously, and shown in Figure 1b, the amount of error increases proportionally with increasing wind speed. Therefore, the amount of error in wind direction should decrease as the wind speed increases. This feature can be seen in Figure 2b: as the wind speed increases, the variance of the differences in wind direction decreases.

[35] The variance of the differences of wind stress is also examined in this idealized case, as shown in Figure 3. At this time there is no comparison to scatterometer wind stress values; however, there are plans to calibrate scatterometers to wind stress. Therefore, the variance of the differences of wind stress is shown here for completeness. The trends seen in the variance of the differences in wind stress are similar to those found in the variance of the differences of U_{10} and of U_{10EN} . As time increases, the amount of variance of the differences of wind stress increases (Figure 3a). The amount of variance of the differences also increases as the wind speed increases (Figure 3b), with a more substantial increase in the highest wind speed group. Because surface stress is primarily dependent on wind shear, there is a nonlinear dependency on wind speed. As shown in equation (5), wind stress (τ) does not increase linearly with the equivalent neutral wind speeds

$$\tau = \rho C_D U_{10EN} |U_{10EN}|, \quad (5)$$

where ρ is the air density and C_D is the neutral drag coefficient.

4. Collocation and Comparison Method

4.1. SeaWinds and SAMOS Collocations

[36] The idealized case results are verified using collocated SeaWinds and SAMOS observations. Because the SeaWinds scatterometer is onboard a polar-orbiting satellite, any given surface location will be sampled on the order of once per day. Therefore, it is reasonable to assume that daily collocated SeaWinds and SAMOS observations can be obtained. Using the collocated observations, the variance due to the temporal and spatial difference between the two observations and the variance due to the data sets can be determined.

[37] As discussed in section 2.2, SeaWinds has up to 76 wind vector cells composing the 1800 km wide observation swath. As SeaWinds passes over a SAMOS vessel, multiple SeaWinds wind vector cells are in close proximity to the 1 min SAMOS observations. Because the closest collocation in both time and space is desired for this study, all of the SeaWinds wind vector cells and all of the SAMOS observations that are within 30 min and 30 km of each other are examined. To find the closest collocation, the combined temporal and spatial difference needs to be determined for each of the observations within the predefined range. Although a temporal difference between two observations is not the same as a spatial difference between two observations, it is possible to combine the two differences by using Taylor's hypothesis, or frozen turbulence. This method, as discussed in section 3.1, allows for a spatial

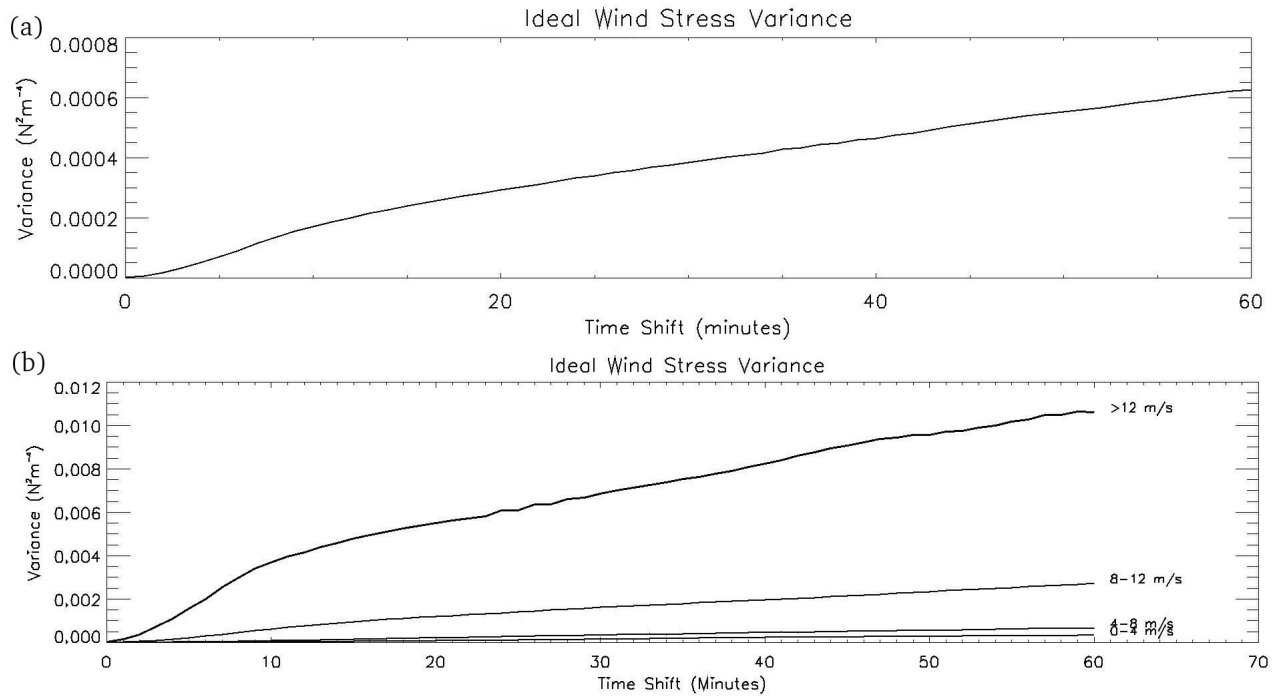


Figure 3. Variance of the differences in wind stress variance as a function of (a) miscollocation in time and (b) miscollocation in time and wind speed.

difference (*space_diff*) to be translated into a temporal difference (*converted_space*). It is also possible to translate a temporal difference into a spatial difference using this same method. However, since the variance of the differences in the idealized case was examined as a function of time, the difference in the SeaWinds and SAMOS observations are examined as a function of time as well for consistency. This translation is accomplished by using equation (6)

$$converted_space = \frac{space_diff}{|U_{sat}|}, \quad (6)$$

where U_{sat} is the SeaWinds-measured wind speed.

[38] Because the spatial difference and the temporal difference are independent of each other, the combined total difference in min (*total_diff*) can be calculated from the root mean square (rms) sum of the converted spatial difference and the temporal difference (*time_diff*). Equation (7) shows this calculation

$$total_diff = \sqrt{time_diff^2 + converted_space^2}. \quad (7)$$

[39] The total difference is calculated for each of the SeaWinds wind vector cells and SAMOS observations within the predefined 30 min and 30 km range. The SeaWinds wind vector cell and the SAMOS observation corresponding to the minimum total difference is considered to be the closest collocation.

[40] An extremely exaggerated example of the collocation procedure can be seen in Figure 4, which shows four wind vector cells and three SAMOS observations. In reality, scatterometer cells within a single pass are within a few

seconds of each other; therefore, a fixed SeaWinds scan time of 10:00 is selected for the shown scatterometer cells. Also for simplicity, only the solid line wind vector cell and the three SAMOS observations will be used in this example to determine the closest collocation. The time differences between the solid SeaWinds wind vector cell and each of the SAMOS observations can be determined by using the reporting times given by the observations. Likewise, the spatial

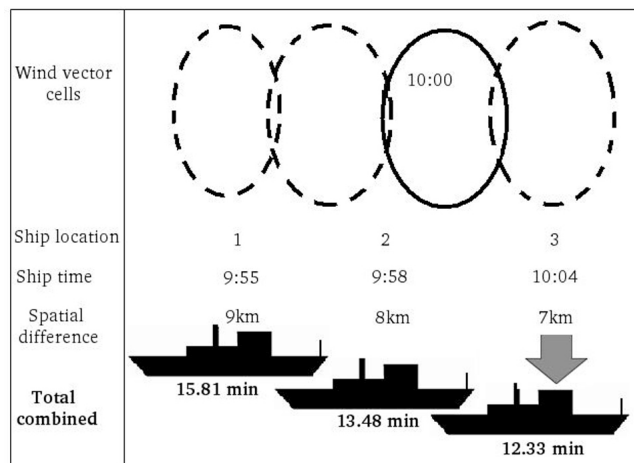


Figure 4. Schematic showing an example of the SeaWinds and SAMOS collocation method using three SAMOS observations and four SeaWinds wind vector cells. The time differences and the spatial differences are combined to find the total difference for each potential collocation. The minimum total difference is determined to be the closest collocation.

differences between the center of the solid SeaWinds wind vector cell and each of the SAMOS observations can be determined by using the given latitudes and longitudes corresponding to the observations. For this example, an assumed constant SeaWinds wind speed of 10 m s^{-1} is used to convert the spatial differences into temporal differences using Taylor's hypothesis (i.e., for ship location 1 the converted space is equal to $9000 \text{ m}/(10 \text{ m s}^{-1} \cdot 60 \text{ s m in}^{-1})$, which equals 15 min). The converted spatial difference can then be added to the temporal difference to find a total combined difference as an RMS sum (i.e., for ship location 1 the total difference is equal to $\sqrt{(5\text{min}^2 + 15\text{min}^2)}$, which equals 15.81 min). This process is repeated for each of the SAMOS observations. The minimum total difference can then be determined (i.e., the ship location with the arrow) and is considered to be the closest collocation in both time and space.

[41] Spatial differences and temporal differences each have an impact on the total difference. As seen in the simplified example in Figure 4, the spatial difference has a larger impact than the temporal difference: the closest collocation corresponds to the smallest spatial difference (ship location 3), not the smallest temporal difference (ship location 2). The relative importance is a function of the actual differences and the wind speed. Since the times of the QuikSCAT observations differ by roughly 4 s, there is little difference in the times. For SAMOS comparisons, the match in time is often excellent ($<30 \text{ s}$), making the distance the bigger factor. Therefore, the collocations chosen are typically the closest in space and very close in time. The outliers occur when the data are very near land, or some of the data are seriously rain contaminated.

[42] Because the SAMOS data are provided every minute, a time-averaging window (t_{win}) for the SAMOS data needs to be defined to ensure the sampling from SAMOS matches the sampling from SeaWinds

$$t_{win} = \frac{\text{footprint}}{|U_{sat}|}, \quad (8)$$

where *footprint* is the footprint size of SeaWinds (*footprint* = 7 km) and U_{sat} is the satellite wind speed for the given collocation. The average SAMOS 10 m EN wind speed and wind direction are calculated within the time-averaging window for comparison to the collocated SeaWinds observation. This process of finding the closest collocation and then calculating the SAMOS time-averaging window and corresponding averaged parameters is done for every SeaWinds overpass.

4.2. SeaWinds and SAMOS Comparisons

[43] After the closest collocation and the associated time-averaging window are determined, the collocated SeaWinds and SAMOS observations can be compared. Although the actual U_{10} , U_{10EN} , wind direction, and wind stress are examined in the idealized case, only the EN wind speed and wind direction can be compared in the real world since SeaWinds currently provides only U_{10EN} and wind direction. As discussed in section 2.2, scatterometers respond to the wind stress. Therefore, the U_{10EN} provided by SeaWinds is a measure of the wind stress (shear), as opposed to the wind

speed at 10 m. Consequently, considering the horizontal motion of the ocean surface in the calculation of the SAMOS U_{10EN} would theoretically provide better comparison data to the SeaWinds observations. To determine if including the ocean surface does or does not improve the comparison between SeaWinds- and SAMOS-measured wind speeds, two average SAMOS 10 m equivalent neutral wind speeds, one without the ocean surface term (U_{10EN}) and one with it (U_{10EN}^*), are calculated using equation (2) from section 2.1 within each of the time-averaging windows for comparison to the collocated SeaWinds observation.

[44] U_{10EN} is determined by setting the ocean surface term (U_{sfc}) equal to zero. U_{10EN}^* includes the horizontal motion of the ocean surface due to ocean waves and currents. The waves and currents data are obtained from model data and are then bilinearly interpolated to the location of the ship. The U_{sfc} term is computed using

$$U_{sfc} = U_{curr} + 0.8U_{orb}, \quad (9)$$

where U_{curr} is the surface current and U_{orb} is the orbital velocity. By including the U_{sfc} term in computing U_{10EN}^* , the wind shear is being accounted for.

[45] Wave data are used to estimate how waves influence the wind shear by modifying the lower boundary condition on velocity. The orbital velocity term (U_{orb}) is used to transform the velocity frame of reference to a fraction of the orbital velocity of the dominant waves [Bourassa, 2004]. The orbital velocity is a function of the significant wave height (H_s) and the corresponding significant wave height period (T_p)

$$U_{orb} = \frac{\pi H_s}{T_p}. \quad (10)$$

[46] The fraction of the orbital velocity that modifies the surface wind is 80% [Bourassa, 2006] and should be removed from the vector wind.

[47] When SeaWinds is compared to U_{10EN}^* , as opposed to U_{10EN} , there are fewer collocated observations because of the limitations of the wave and current data: the data does not extend past 69.5°N/S and does not exist very close to land. Therefore, if the closest collocation corresponds to the SAMOS vessel being close to the coastline, then there will be no model data available. Only the collocated observations that have both waves and currents available are examined and compared in this study.

[48] Additional collocations are removed from the collocated data set because the differences are far too large to be due to random errors: the collocated data are likely on different sides of an atmospheric front, the SAMOS data are in error, or the scatterometer wind could be seriously rain impacted but improperly flagged. As discussed in section 2.3, the SAMOS data that are used in this study have not been visually quality controlled. Spikes in wind speed that would be determined as flawed by a visual inspection could pass the automated quality control and therefore be present in this data set. The difference between the collocated wind speeds should be well within 5 m s^{-1} and the difference between the collocated wind directions should be no more than 45° for correctly selected ambiguities. The wind direction constraint eliminates collocated observations for

which ambiguity errors are associated with large errors in direction. There are viewing geometries in which much smaller ambiguity directions can be expected: these smaller errors are not removed from the comparison data set.

[49] Once the acceptable collocations have been determined, U_{10EN} , U_{10EN}^* , and the SAMOS-measured wind directions can be compared with SeaWinds. For each of the collocations, the total difference in min between the SeaWinds and SAMOS observations is determined (equation (7)). The total variance (σ_j^2) of the differences between the SeaWinds-measured wind speed and the SAMOS-averaged 10 m EN wind speed (ΔU_{ij}) is calculated using all of the collocations with a j min total time difference in equation (11)

$$\sigma_j^2 = \frac{1}{N_j - 1} \sum_{i=1}^{N_j} (\Delta U_{ij})^2, \quad (11)$$

where N is the number of observations with a j min time shift. The same method is used for calculating the total variance of the differences between the SeaWinds-measured and the SAMOS-averaged wind directions. The total variance of the differences is calculated for both wind speed comparison data sets as a function of the total temporal difference to determine the effect of including or not including the ocean surface. The total variance of the wind direction differences is also calculated as a function of the total temporal difference. Each of the total variances of the differences is also examined as a function of wind speed to determine the variance associated with the data sets versus the variance associated with the temporal and spatial difference between the observations.

5. Results

[50] Figure 5 shows scatterplots of the collocated SeaWinds-measured winds compared to U_{10EN} (Figure 5a), to U_{10EN}^* (Figure 5b), and to SAMOS-measured wind directions (Figure 5c) that meet the constraints identified in section 4. Initially, there were 1662 collocations found when the ocean surface term was ignored; when the ocean surface term was included, the total number of collocations was reduced to 1575. If wind speed (wind direction) was the only constraint for removing outliers, 62 (292) additional collocations would be removed. Ultimately, 1255 collocations were deemed as acceptable collocations. When the ocean surface term is included in the calculation for the 10 m EN wind speed, the best fit line between the two data sets is closer to a one-to-one correlation. These results suggest that including the ocean surface term provides a better 10 m EN wind speed for comparison.

[51] For each data set, the total variance of the differences associated with all collocations with a j min temporal (equivalent) difference is examined. Unfortunately, calculating the variance of the differences associated with each of these temporal 1 min bins produces extremely noisy results. The excessive noise makes it difficult to extract any discernible information about the variance of the differences. Therefore, a 15 min running mean, or boxcar filter, is applied to smooth the total variance of the differences for each data set (Figure 6). One notable feature in Figure 6a is that the total variance of the differences of U_{10EN}^* is slightly

less than the total variance of the differences of U_{10EN} . U_{10EN} considers the atmospheric contribution to shear, but ignores the ocean's motion. However, by including the ocean surface term in U_{10EN}^* , the shear within that layer is more appropriately represented for calculating stress (see section 4.2). The lower total variance of the differences when surface motion is considered supports the idea that scattermeters respond more to wind shear than to earth-relative air motion [Cornillon and Park, 2001; Kelly et al., 2001; Chelton et al. 2004].

[52] The other notable feature Figure 6a is the trend in the total variance of the differences. Initially, the total variance of the differences in wind speed (Figure 6a) decreases as the time (equivalent) difference increases. After approximately a 30 min time (equivalent) difference, the total variance of the differences begins to increase as the time (equivalent) difference increases. On the basis of the idealized case wind speed results, a general increasing trend should be seen for all time differences. The trend in the total variance of the differences in wind direction (Figure 6b) has a general increasing pattern as the time shift increases, which agrees better with the results found in the idealized case. To determine the cause of the initial decreasing trend found in the collocated wind speed results and to further verify the idealized case results, the total variance of the differences is separated into three wind speed groups: 0–4, 4–7, and 7–12 m s^{-1} . Instead of calculating the variance of the differences of all of the collocations for each 1 min time (equivalent) difference, the variance of the differences of the collocations within a certain wind speed range for each 1 min time (equivalent) difference is calculated.

[53] The total variance of the differences, separated into three wind speed groups, is shown for U_{10EN} (Figure 7). If there are fewer than ten collocations within a given 1 min time difference, the sample size is considered to be too small and the total variance of the differences associated with that time difference is not calculated. The lowest wind speed group, 0–4 m s^{-1} , is not consistent with the idealized case results. There are several factors that could influence the results in this wind speed group. The first consideration is that scattermeters have greater difficulty accurately measuring wind speeds less than 3 m s^{-1} primarily because of ambiguity selection errors [Bourassa et al., 2003]. Another problem with this lowest wind speed group is that it is associated with the largest time-averaging window when Taylor's hypothesis is applied. For example, a 3 m s^{-1} wind speed corresponds to a time-averaging window of 39 min; in comparison, a 6 m s^{-1} wind speed corresponds to a 19 min time-averaging window. It is assumed that the statistics of the wind speeds remain the same within the time-averaging window; however, this is not a reasonable assumption for large time-averaging windows because wind speed changes rapidly with time. Conversely, for very high wind speeds, the time averaging window determined using Taylor's hypothesis is too short to have sufficient sampling when sampled in 1 min intervals. All wind speeds examined in this study correspond to an adequately large time averaging window; therefore, the threshold when the wind speed becomes too high cannot be determined in this analysis. The problems associated with the lowest wind speed group make it difficult to determine any significant meaning in the total variance of the differences for that speed range. Therefore,

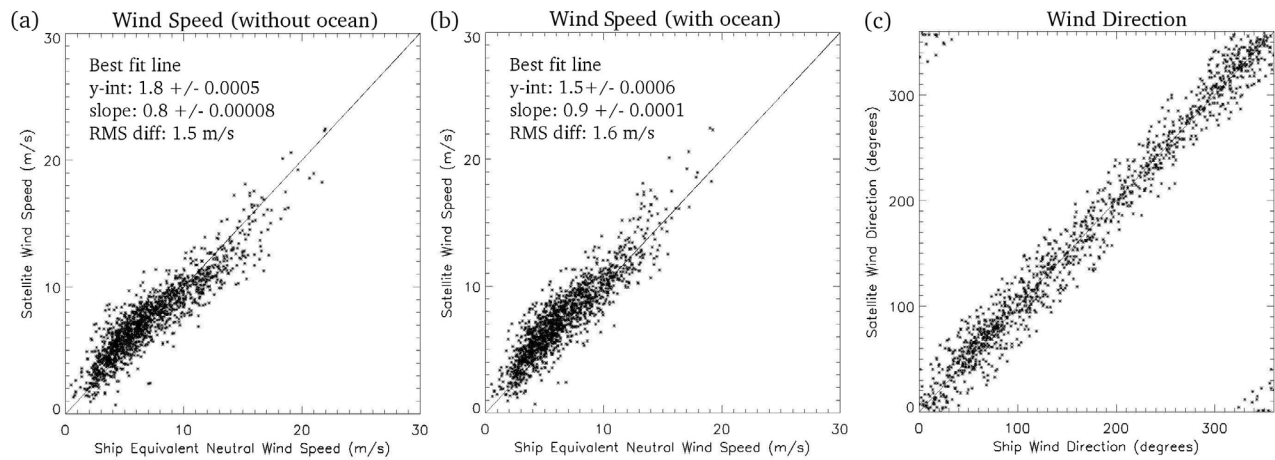


Figure 5. Collocated SeaWinds-measured winds versus (a) adjusted SAMOS 10 m equivalent wind speeds calculated by neglecting the ocean surface term, (b) adjusted SAMOS 10 m equivalent wind speeds calculated by including the ocean surface term, and (c) SAMOS-measured wind direction. Each of these collocations have wave and current data available, less than a 5 m s^{-1} wind speed difference, and less than a 45° difference in wind direction.

only the total variance of the differences associated with wind speeds greater than or equal to 4 m s^{-1} are further examined.

[54] The curves seen in Figure 7 represent the total variance of the differences in U_{10EN} , which is composed of the variance in the data sets as well as the variance associated with the temporal and spatial difference between the two

observations. The variance associated with the data sets should be relatively constant, whereas the variance associated with the temporal and spatial difference should gradually increase as the time (equivalent) difference increases, as shown in the idealized case. The relatively constant total variance that is seen from a 0 to 25 min time (equivalent) difference shows the time differences for which the variance

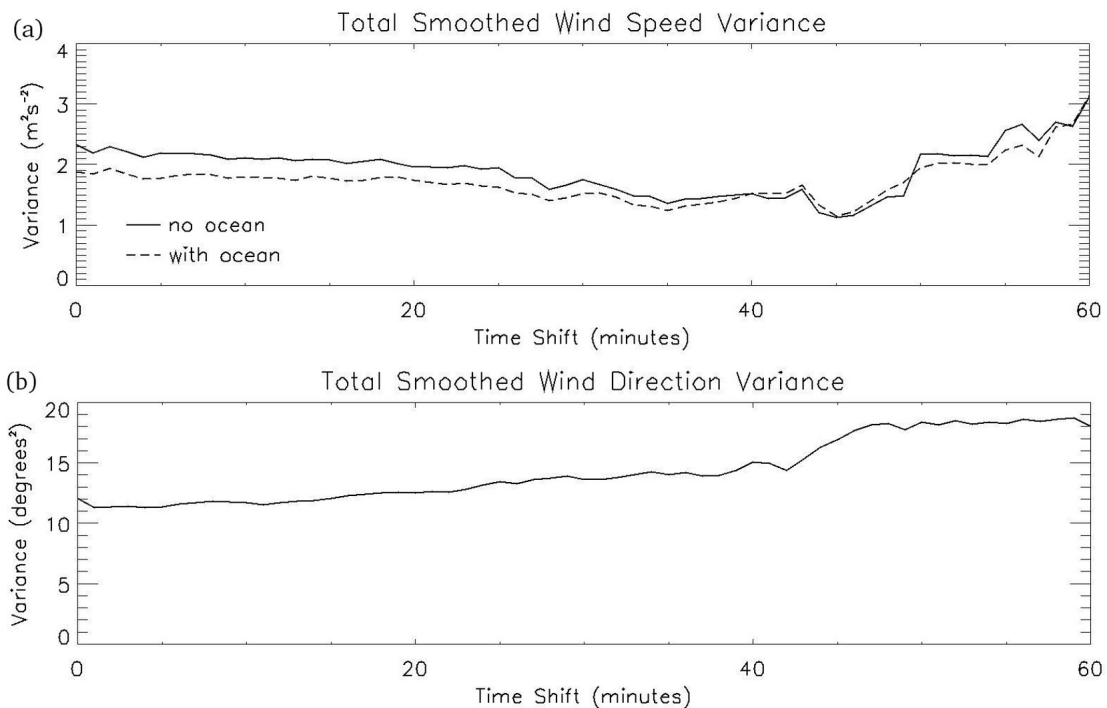


Figure 6. Total variance of the differences (a) in the adjusted SAMOS 10 m EN wind speed excluding the ocean surface term (solid line) and including the ocean surface term (dashed line) and (b) in wind direction for all of the collocated observations for each 1 min time difference, with a 15 min running mean filter applied.

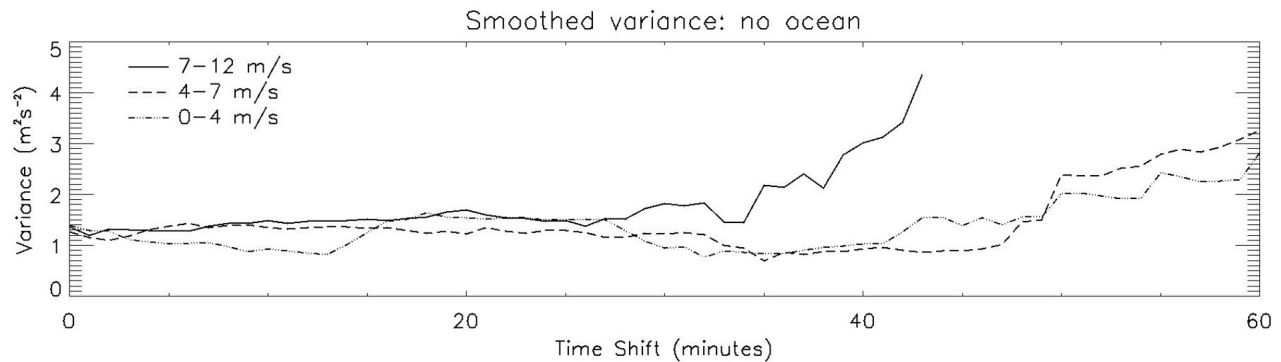


Figure 7. Total variance of the differences of the collocated wind speed observations, excluding the ocean surface term, within the 0–4 (dash-dotted line), 4–7 (dashed line), and 7–12 m s^{-1} (solid line) wind speed group for each 1 min time difference, with a 15 min running mean filter applied.

associated with observational errors in the data sets dominates the variance associated with the temporal and spatial differences between the two observations. The total variance found in this region is representative of the total observational error variance associated with the two collocated data sets: SeaWinds and SAMOS. Therefore, it can be deduced, from Figure 7, that this total variance between well-collocated SeaWinds and SAMOS observations for $7 < U_{10} < 12 \text{ m s}^{-1}$ is approximately $1.5 \text{ m}^2 \text{ s}^{-2}$, which corresponds to an approximate standard deviation of 1.2 m s^{-1} . For $4 < U_{10} < 7 \text{ m s}^{-1}$, the total variance associated with the two data sets is approximately $1.0 \text{ m}^2 \text{ s}^{-2}$.

[55] After a 25 min time (equivalent) difference, the total variance of the differences in Figure 7 gradually increases as the time (equivalent) difference increases. This gradual increase occurs because the variance of the differences associated with the temporal and spatial difference between the two observations is no longer dominated by the variance associated with the two collocated data sets. Therefore, after a 25 min time (equivalent) difference, the variance of the differences associated with the temporal and spatial difference between two observations begins to have an impact on the total observed variance of the differences. Also of note in Figure 7 is that the total variance of the differences associated with the 7–12 m s^{-1} wind speed group is greater

than the total variance of the differences associated with the 4–7 m s^{-1} wind speed group. As in the idealized case, larger wind speeds correspond to larger total variances in the wind speed differences.

[56] If the variance associated with the data sets was added to the idealized case temporal variance found in section 3.2, then theoretically, the resulting total variance of the differences would look similar to that shown in Figure 7. The idealized total variance of the differences, along with the individual variance components, is shown in Figure 8 (solid line) for the idealized 4–7 m s^{-1} wind speed group. Figure 8 shows a relatively constant total variance of the differences until approximately a 10 min time difference, followed by a gradual increase in the total variance of the differences. This increase occurs at a smaller time difference compared to the increase seen at 25 min in Figure 7. Although the idealized case and the real world are not expected to be exactly the same, this much difference between the two was not anticipated. Therefore, further investigation is required.

[57] Examining the different elements within each wind speed group in the real world reveals an unexpected trend in the wind speed distributions as the time difference increases. Figure 9 shows the wind speed associated with the median, 25th percentile, and 75th percentile of the 4–7 m s^{-1} wind speed group for time (equivalent) differences from 0 to

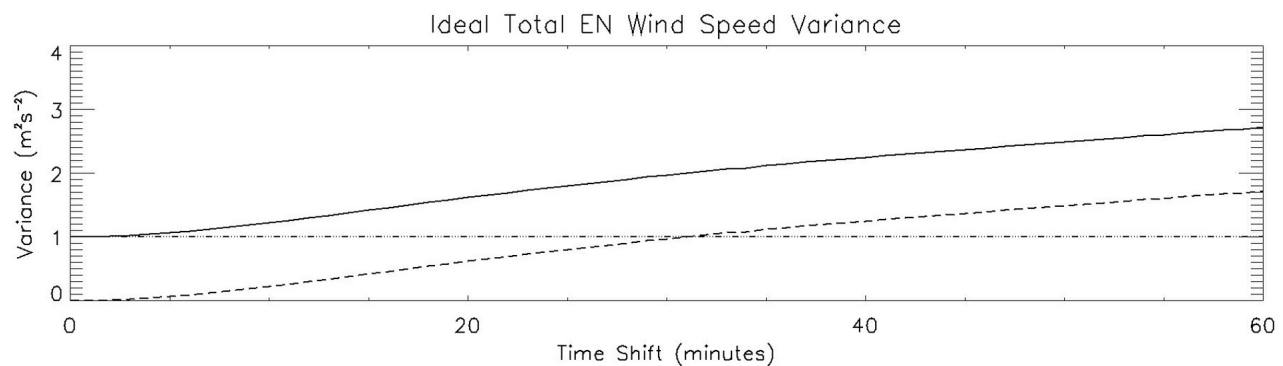


Figure 8. The idealized wind speed case temporal variance (dashed line) is added to the variance associated with the data sets for the 4–7 m s^{-1} wind speed group (dash-dotted line) to obtain the idealized case total variance of the differences (solid line).

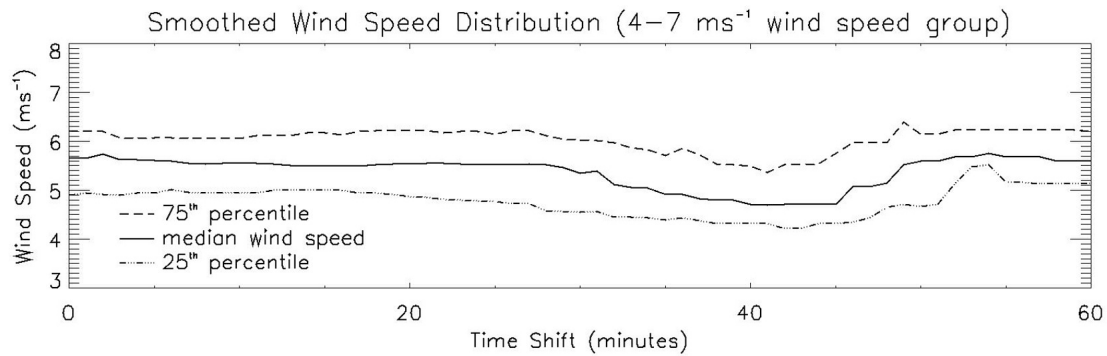


Figure 9. Median (solid line), 25th percentile (dash-dotted line), and 75th percentile (dashed line) wind speed associated with the $4\text{--}7\text{ m s}^{-1}$ wind speed group for each 1 min time difference, with a 15 min running mean filter applied.

60 min. For small time (equivalent) differences (<20 min), all wind speeds within the predefined wind speed range are uniformly represented. Then as the time difference increases to a 45 min time (equivalent difference, the amount of wind speeds at the lower end of the predefined wind speed range increases while the amount of wind speeds at the upper end of the predefined wind speed range decreases. As discussed and shown before, lower wind speeds are associated with a lower amount of variance; therefore, the change in wind speed distribution with increasing time differences results in a reduced variance. For effective time differences less than roughly 25 min (and speed bin widths of 3 or 4 m s^{-1}), the decreased variance due to the changing wind speed distribution approximately compensates for the increased variance of the differences due to increasing time differences; therefore, the variance associated with the data sets remains the dominating term for an extended period of time differences, until roughly 25 min. After 25 min time (equivalent) difference, the variance due to the increasing time difference becomes dominant. For 45 to 60 min time (equivalent) time differences, the wind speed distribution is seen to increase. This region is based on relatively few points, however, they are the points used in Figures 6, 7, 10, and 11. The increase in wind speed distribution contributes to the increase in the variance of the differences; however, the dominant factor

remains the increase in time difference. It is expected that if the wind speed groups defined in the real world were smaller (e.g., 1 m s^{-1} bins), then the resulting total variance of the differences would be much closer to that seen in the idealized case total variance of the differences (Figure 8). Unfortunately, this study does not have enough data for smaller wind speed bins to be represented adequately; about 3 times the amount of data would be required.

[58] The total variance of the differences in $U_{10\text{EN}}^*$ separated into wind speed groups is shown in Figure 10. Once again, the total variance of the differences is not calculated for time differences containing fewer than 10 collocations. Because of the problems previously discussed respective to the lowest wind speed group, $0\text{--}4\text{ m s}^{-1}$, only the variance of the differences associated with the $4\text{--}7$ and $7\text{--}12\text{ m s}^{-1}$ wind speed groups are shown in Figure 10. Qualitatively, the total variance of the differences of $U_{10\text{EN}}^*$ is similar to the total variance of the differences of $U_{10\text{EN}}$. A relatively constant total variance of the differences is seen initially until roughly a 25 min time (equivalent) difference because of the variance associated with the data sets dominating the variance associated with the temporal and spatial difference between the observations. The gradual increase in the total variance of the differences after about a 25 min time (equivalent) difference is seen because the variance of the

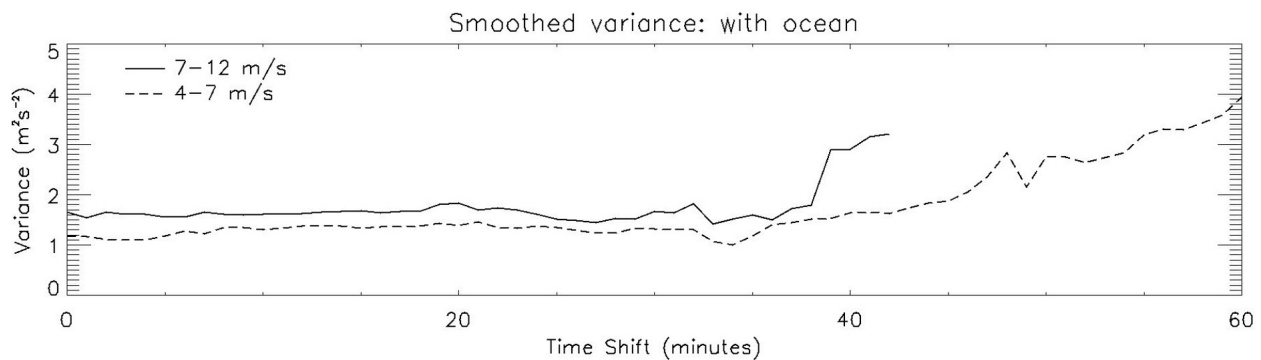


Figure 10. Total variance of the differences of the collocated wind speed observations, including the ocean surface term, within the $4\text{--}7$ (dashed line) and $7\text{--}12\text{ m s}^{-1}$ (solid line) wind speed group for each 1 min time difference, with a 15 min running mean filter applied.

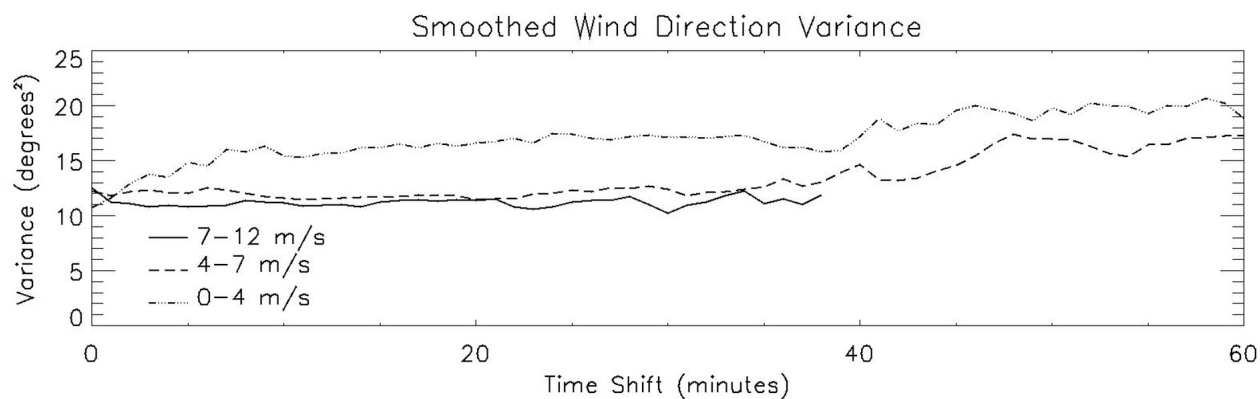


Figure 11. Total variance of the differences of the collocated wind direction observations within the 0–4 (dash-dotted line), 4–7 (dashed line), and 7–12 m s^{-1} (solid line) wind speed group for each 1 min time difference, with a 15 min running mean filter applied.

differences associated with the temporal and spatial difference between observations is no longer dominated by the variance associated with the data sets. Also, the larger wind speed group has a higher total variance associated with it, which agrees with the previously discussed results.

[59] Figure 11 shows the total variance of the differences in wind direction separated into the three wind speed groups. Although the 0–4 m s^{-1} wind speed group is known to have issues associated with it, it is shown in Figure 11 for reference. As with the variance of the differences in wind speed, for each wind speed group the variance of the differences in wind direction is relatively constant until approximately a 25 min time (equivalent) difference. The total variance of the data sets can be determined from the relatively constant region as approximately 12 deg^2 for $4 < U_{10} < 7 \text{ m s}^{-1}$ and approximately 10 deg^2 for $7 < U_{10} < 12 \text{ m s}^{-1}$. After the 25 min time (equivalent) difference, the variance of the differences in wind direction is seen to gradually increase since the variance associated with the data sets is no longer the dominant term. Qualitatively, the results here agree well with the results from the idealized case: for greater wind speeds the total variance of the differences in wind direction decreases.

6. Summary

[60] The variance of the differences in wind speed and wind direction associated with the temporal and spatial difference between two well-collocated ship and satellite wind observations, as well as the variance associated with observational errors in these data sets, is determined. The satellite data were obtained from the SeaWinds scatterometer onboard the QuikSCAT satellite. The ship wind speed and direction data were obtained from the Shipboard Automated Meteorological and Oceanographic System (SAMOS) initiative. The SAMOS measured wind speeds were converted into 10 m Equivalent Neutral (EN) wind speeds using a modified log wind profile.

[61] The variance of the differences in actual wind speed (U_{10}), 10 m EN wind speeds ($U_{10\text{EN}}$), wind direction, and stresses associated with a temporal difference between two observations is first examined in an idealized case using

only SAMOS data. The analysis shows that the total variance of the differences in $U_{10\text{EN}}$ is slightly less than the variance of the differences in U_{10} for low to moderate wind speeds, but larger for greater wind speeds. For unstable conditions, $U_{10\text{EN}}$ is greater than U_{10} , and the variability in wind increases with increasing wind speed. For low to moderate wind speeds, changes in $U_{10\text{EN}}$ due to atmospheric stability offset changes in wind speeds. For larger wind speeds, however, the changes due to stability are reduced and cannot compensate for the greater variability associated with larger wind speeds. The idealized case shows that for the actual wind speed, EN wind speed, and wind direction, as the time difference between two observations increases, the amount of variance of the differences increases. Higher wind speeds are also found to be associated with a larger amount of variance of the differences in wind speeds and a smaller amount of variance of the differences in wind directions.

[62] The results from the idealized case are verified using collocated SeaWinds and SAMOS data. The changes associated with considering the motion of the ocean surface ($U_{10\text{EN}}^*$) are examined in the comparison of SAMOS-measured wind speeds to 10 m EN wind speeds ($U_{10\text{EN}}$). Modeled waves and currents data are used to represent the ocean surface. The total variance of the differences in the data set that includes the ocean surface data and the data set that does not include these data are compared. The data set using the ocean surface data is found to be a better match to SeaWinds.

[63] The total variance of the differences in wind speed and direction associated with the collocations is examined as a function of the temporal and spatial difference between the observations as well as a function of wind speed. As in the idealized case, the higher wind speeds are found to correspond to a larger total variance of the differences in wind speed and smaller total variance of the differences in wind direction. A relatively constant total variance of the differences in wind speed and direction of approximately $1.5 \text{ m}^2 \text{ s}^{-2}$ and 10 deg^2 for $7 < U_{10} < 12 \text{ m s}^{-1}$ and $1.0 \text{ m}^2 \text{ s}^{-2}$ and 12 deg^2 for $4 < U_{10} < 7 \text{ m s}^{-1}$ is found until roughly a 25 min (equivalent) time difference. This initial constant variance of the differences represents the time differences for which the variance associated with observational error in the data sets is

the dominant term in the total variance. After a 25 min (equivalent) time difference, the variance of the differences gradually increases as the time difference increases, as seen in the idealized case. This increasing total observational variance of the differences is due to the variance associated with the spatial and temporal difference between the observations; the variance associated with observational errors is no longer the dominating term and therefore the total amount of variance of the differences is no longer constant (it is not offset by the changing wind speed distribution). It can then be deduced that if collocated ship and satellite observations have greater than a 25 min (equivalent) difference, the variance associated with the temporal and spatial difference needs to be accounted for in the total variance of the differences; however, for collocations with less than a 25 min (equivalent) difference, and bin sizes of 3 to 5 m s⁻¹, the variance associated with only the data sets needs to be considered for the total variance of the differences.

[64] **Acknowledgments.** The version 3 SeaWinds wind data were obtained from the Remote Sensing Systems. The SAMOS data were provided by the Research Vessel Surface Meteorology Data Center. The ocean current data were obtained from the NOAA Ocean Surface Current Analyses - Real Time (OSCAR) global data set and the ocean wave data were obtained from the NOAA WAVEWATCH III (NWW3) global ocean wave model. Support for this research came from the NOAA Climate Observation Division (COD) and the NASA Ocean Vector Winds Science Team (OVWST).

References

- Bonjean, F., and G. S. E. Lagerloef (2002), Diagnostic model and analysis of the surface currents in the tropical Pacific ocean, *J. Phys. Oceanogr.*, **32**, 2938–2954.
- Bourassa, M. A. (2004), An improved sea state dependency for surface stress derived from in situ and remotely sensed winds, *Adv. Space Res.*, **33**, 1136–1142, doi:10.1016/S0273-1177(03)00753-1.
- Bourassa, M. A. (2006), Satellite-based observations of surface turbulent stress during severe weather, in *Atmosphere-Ocean Interactions*, vol. 2, edited by W. Perrie, pp. 35–52, Wessex Inst. of Technol. Press, Southampton, UK.
- Bourassa, M. A., D. G. Vincent, and W. L. Wood (1999), A flux parameterization including the effects of capillary waves and sea state, *J. Atmos. Sci.*, **56**, 1123–1139, doi:10.1175/1520-0469(1999)056<1123:AFPITE>2.0.CO;2.
- Bourassa, M. A., D. M. Legler, J. J. O'Brien, and S. R. Smith (2003), SeaWinds validation with research vessels, *J. Geophys. Res.*, **108**(C2), 3019, doi:10.1029/2001JC001028.
- Bourassa, M. A., E. Rodriguez, and R. Gaston (2010a), NASA's Ocean Vector Winds Science Team workshops, *Bull. Am. Meteorol. Soc.*, **91**, 925–928, doi:10.1175/2010BAMS2880.1.
- Bourassa, M. A., et al. (2010b), Remotely sensed winds and wind stresses for marine forecasting and ocean modeling, in *Proceedings of the OceanObs'09: Sustained Ocean Observations and Information for Society Conference*, vol. 2, edited by J. Hall, D. E. Harrison, and D. Stammer, Eur. Space Agency, Venice, Italy, in press.
- Bradley, F., and C. Fairall (2006), A guide to making climate quality meteorological and flux measurements at sea, *NOAA Tech. Memo. OAR PSD-311*, Earth Syst. Res. Lab., Boulder, Colo.
- Chelton, D. B., M. G. Schlax, M. H. Freilich, and R. F. Milliff (2004), Satellite measurements reveal persistent small-scale features in ocean winds, *Science*, **303**, 978–983, doi:10.1126/science.1091901.
- Chen, G. (2000), On the choice of space and time windows for the comparison of altimeter-derived sea surface wind speeds with in situ measurements, *Int. Arch. Photogramm. Remote Sens.*, **33**, 112–118.
- Cornillon, P., and K. A. Park (2001), Warm core ring velocities inferred from NSCAT, *Geophys. Res. Lett.*, **28**, 575–578, doi:10.1029/2000GL011487.
- Dobson, E., F. Monaldo, and J. Wilkerson (1987), Validation of Geosat altimeter-derived wind speeds and significant wave heights using buoy data, *J. Geophys. Res.*, **92**, 10,719–10,731, doi:10.1029/JC092iC10p10719.
- Draper, D. W., and D. G. Long (2004), Evaluating the effect of rain on SeaWinds scatterometer measurements, *J. Geophys. Res.*, **109**, C02005, doi:10.1029/2002JC001741.
- Ebuchi, N., H. C. Graber, and M. J. Caruso (2002), Evaluation of wind vectors observed by QuikSCAT/SeaWinds using ocean buoy data, *J. Atmos. Oceanic Technol.*, **19**, 2049–2062, doi:10.1175/1520-0426(2002)019<2049:EOWVOB>2.0.CO;2.
- Freilich, M. H., and R. S. Dunbar (1999), The accuracy of the NSCAT 1 vector winds: Comparisons with National Data Buoy Center buoys, *J. Geophys. Res.*, **104**, 11,231–11,246, doi:10.1029/1998JC900091.
- Huddleston, J. N., and M. W. Spencer (2001), SeaWinds: The QuikSCAT wind scatterometer, *IEEE Proc. Aerospace Conf.*, **4**, 1825–1831.
- Kara, A. B., A. J. Wallcraft, and M. A. Bourassa (2008), Air-sea stability effects on the 10 m winds over the global ocean: Evaluations of air-sea flux algorithms, *J. Geophys. Res.*, **113**, C04009, doi:10.1029/2007JC004324.
- Kelly, K. A., S. Dickinson, M. J. McPhaden, and G. C. Johnson (2001), Ocean currents evident in satellite wind data, *Geophys. Res. Lett.*, **28**, 2469–2472, doi:10.1029/2000GL012610.
- Kent, E. C., P. G. Challenor, and P. K. Taylor (1999), A statistical determination of the random observational errors present in voluntary observing ships meteorological reports, *J. Atmos. Oceanic Technol.*, **16**, 905–914, doi:10.1175/1520-0426(1999)016<0905:ASDOTR>2.0.CO;2.
- Liu, W. T. (2002), Progress in scatterometer application, *J. Oceanogr.*, **58**, 121–136, doi:10.1023/A:1015832919110.
- Liu, W. T., and X. Xie (2006), Measuring ocean surface wind from space, in *Remote Sensing of the Marine Environment: Manual of Remote Sensing*, vol. 6, 3rd ed., edited by J. Gower, pp. 149–178, Am. Soc. for Photogramm. and Remote Sens., Bethesda, Md.
- Long, D. G. (2002), High resolution wind retrieval from SeaWinds, *Proc. Int. Geosci. Remote Sens. Symp.*, **2**, 751–753, doi:10.1109/IGARSS.2002.1025662.
- Monaldo, F. (1988), Expected differences between buoy and radar altimeter estimates of wind speed and significant wave height and their implications on buoy-altimeter comparisons, *J. Geophys. Res.*, **93**, 2285–2302, doi:10.1029/JC093iC03p02285.
- Pierson, W. J. (1990), Examples of, reasons for, and consequences of the poor quality of wind data from ships for the marine boundary layer: Implications for remote sensing, *J. Geophys. Res.*, **95**, 13,313–13,340, doi:10.1029/JC095iC08p13313.
- Portabella, M., and A. Stoffelen (2009), On scatterometer ocean stress, *J. Atmos. Oceanic Technol.*, **26**, 368–382, doi:10.1175/2008JTECH0578.1.
- Ross, D. B., V. J. Cardone, J. Overland, R. D. McPherson, W. J. Pierson Jr., and T. Yu (1985), Oceanic surface winds, *Adv. Geophys.*, **27**, 101–140, doi:10.1016/S0065-2687(08)60404-5.
- Smith, S. R., M. A. Bourassa, and R. J. Sharp (1999), Establishing more truth in true winds, *J. Atmos. Oceanic Technol.*, **16**, 939–952, doi:10.1175/1520-0426(1999)016<0939:EMTITW>2.0.CO;2.
- Smith, S. R., J. Rettig, J. Rolph, J. Hu, E. C. Kent, E. Schulz, R. Vereen, S. Rutz, and C. Paver (2010), The data management system for the Shipboard Automated Meteorological and Oceanographic System (SAMOS) initiative, in *Proceedings of the OceanObs'09: Sustained Ocean Observations and Information for Society Conference*, vol. 2, edited by J. Hall, D. E. Harrison, and D. Stammer, Eur. Space Agency, Venice, Italy, in press.
- Stoffelen, A. (1998), Toward the true near-surface wind speed: Error modeling and calibration using triple collocation, *J. Geophys. Res.*, **103**, 7755–7766, doi:10.1029/97JC03180.
- Taylor, G. I. (1938), The spectrum of turbulence, *Proc. R. Soc. A*, **67**, 16–20.
- Weissman, D. E., K. L. Davidson, R. A. Brown, C. A. Friehe, and F. Li (1994), The relationship between the microwave radar cross section and both wind speed and stress: Model function studies using Frontal Air-Sea Interaction Experiment data, *J. Geophys. Res.*, **99**, 10,087–10,108, doi:10.1029/93JC03371.
- Weissman, D. E., M. A. Bourassa, and J. Tongue (2002), Effects of rain rate and wind magnitude on SeaWinds scatterometer wind speed errors, *J. Atmos. Oceanic Technol.*, **19**, 738–746, doi:10.1175/1520-0426(2002)019<0738:EOORAW>2.0.CO;2.

M. A. Bourassa, Center for Ocean-Atmospheric Prediction Studies, Florida State University, 2035 E. Paul Dirac Dr., 200 RM Johnson Bldg., Tallahassee, FL 32306, USA. (bourassa@coaps.fsu.edu)
J. C. May, QinetiQ North America, Bldg. 1009, Stennis Space Center, MS 39529, USA. (jmay@coaps.fsu.edu)